Reaction Mechanisms

Mechanism of the Norrish–Yang Photocyclization Reaction of an Alanine Derivative in the Singlet State: Origin of the Chiral-Memory Effect**

Adalgisa Sinicropi, Frédérique Barbosa, Riccardo Basosi, Bernd Giese, and Massimo Olivucci**

The asymmetric synthesis of enantiomerically pure α-amino acids is a major topic of modern peptide chemistry.[1–8] For the development of new peptidomimetics, proline derivatives are

[*] Dr. F. Barbosa,[+] Prof. Dr. B. Giese
Department of Chemistry
St. Johanns-Ring 19, 4056 Basel (Switzerland)
Fax: (+41) 61-267-1105
E-mail: bernd.giese@unibas.ch
Dr. A. Sinicropi, Prof. Dr. R. Basosi, Prof. Dr. M. Olivucci
Dipartimento di Chimica
Università degli Studi di Siena
via Aldo Moro, 53100 Siena (Italy)
Fax: (+39) 0577-234-278
E-mail: olivucci@unisi.it
[+] Current address:
Cerep
128 rue Danton, 92500 Rueil Malmaison (France)

[**] This work was supported by the HFSP (RG 0229/2000M), the Università di Siena (Progetto di Ateneo A.A. 00/04), FIRB project no. RBAU01EPMR, and the Swiss National Science Foundation.

Supporting information for this article (coordinates and energies of all optimized structures) is available on the WWW under http://www.angewandte.org or from the author.

  DOI: 10.1002/ange.200461898

of particular importance.[9] Recently, Giese et al.[10] reported a stereospecific photochemical route to proline derivatives by a singlet Norrish–Yang photocyclization reaction of the alanine derivative **1**, which leads to the diastereoisomers **2**, ent-**2**, **3**, and ent-**3** ("ent" denotes the enantiomer of the compound indicated; Scheme 1). In the presence of the triplet quencher and singlet sensitizer naphthalene, with benzene as the solvent, the photocyclization yielded isomer **2** (92% *ee*) with the *cis* configuration as the major product, with retention of configuration at the α carbon atom. The minor *trans* isomer **3** (*cis*/*trans* 85:15) was also formed with 88% *ee*. This reaction is one of the few remarkable examples of the photochemical "chiral-memory effect".[11] Furthermore, it represents an example of the exploitation of light energy to drive asymmetric synthesis.

To understand this memory effect we carried out ab initio CASPT2//CASSCF[10,8][12–17] computations to map the photochemical reaction pathway of the alanine-derivative model **4**. The results of the calculations are shown in Figure 1. Upon photoexcitation, one electron of the oxygen lone pair is

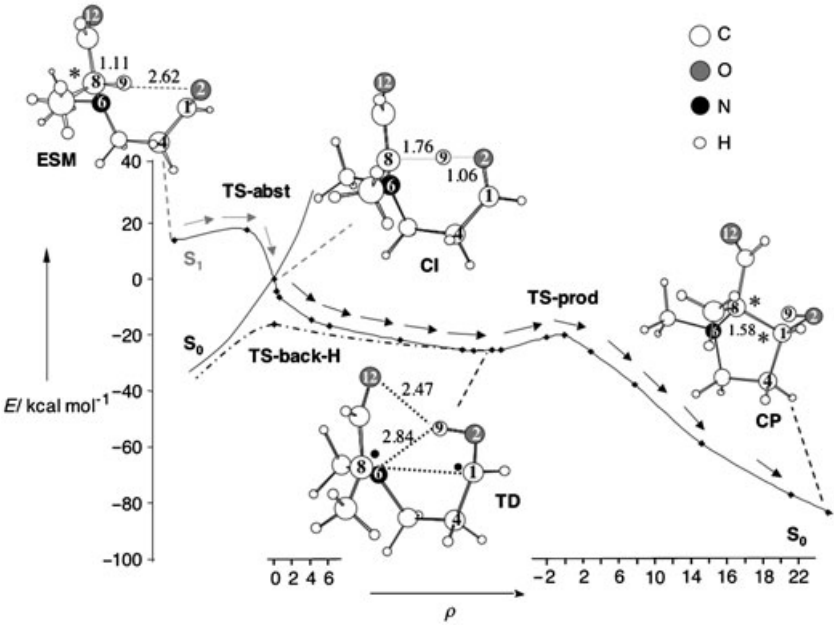

Figure 1. Energy profiles along the S_1 and S_0 reaction coordinate for the intramolecular hydrogen-atom abstraction, hydrogen-atom back transfer (dashed–dotted line), and the cyclization of compound **4**. The chiral centers are labeled with an asterisk.

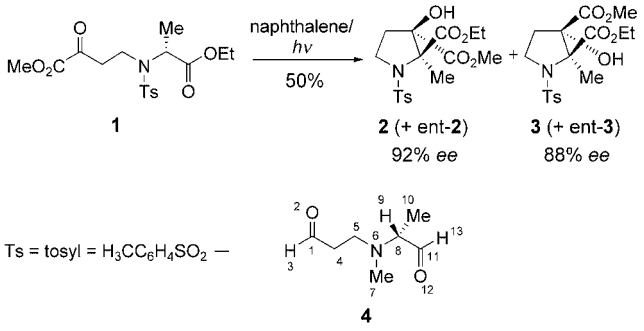

Scheme 1. Singlet Norrish–Yang photocyclization reaction of the alanine derivative **1**; alanine-derivative model **4**.

promoted to the π* orbital of the C1=O2 bond. The computed excitation energy for the singlet n–π* excitation is 98.1 kcal mol^{-1}. After photoexcitation, the molecule relaxes to the stable excited-state (S_1) conformation **ESM** (Figure 1) with an O2–H9 distance of 2.62 Å, which is comparable to the distance of 2.69 Å observed in the 1,5-hydrogen-atom abstraction of solid-state compounds by Ihmels and Scheffer[18] and to the average value of 2.61 ± 0.07 Å observed for 14 ketones whose crystal structures were determined.[19]

The hydrogen-atom transfer from C8 to O2 is controlled by the transition-state structure **TS-abst** (Figure 1), which is located 6.8 kcal mol^{-1} in energy above **ESM** and which connects this intermediate to a conical intersection **CI** between the excited-state S_1 and ground-state S_0 potential-energy surfaces. At the transition state of the H abstraction the distance between the oxygen atom O2 and the hydrogen atom H9 is 1.24 Å, and the distance between the carbon atom C8 and the hydrogen atom H9 is 1.33 Å.

It is generally accepted that in photochemical reactions conical-intersection structures play a role similar to that of transition states in thermal reactions.[20,21] Indeed, these structures provide extremely efficient channels for the decay of the excited-state species to the ground state.

The molecular motion that prompts the $S_1 \rightarrow S_0$ decay occurs along the so-called "branching" plane, which is defined by the coordinates $\mathbf{X_1}$ and $\mathbf{X_2}$ (Figure 2). Any molecular deformation along this plane lifts the S_1/S_0 degeneracy at the intersection. Thus, the analysis of $\mathbf{X_1}$ and $\mathbf{X_2}$ provides useful information about the chemical event mediated by the conical-intersection structure. It is apparent that at the conical intersection **CI** (Figure 1) the hydrogen-atom transfer is almost complete and that an sp^2 radical center has been generated at C8. The plot of the $\mathbf{X_1}$ and $\mathbf{X_2}$ vectors (Figure 2) clearly indicates that the decay leads exclusively to a diradical intermediate or to the original reactant. Indeed, it can be seen that there are no torsional components to prompt twisting about the N6–C8 or C1–C4 bonds accompanied by loss of stereoselectivity at C8 or lack of facial selectivity during the attack at C1.

Consistent with this analysis, the computed paths indicate that the evolution following the decay occurs according to two routes. One of these routes leads back to the starting material, as back transfer of the hydrogen atom may occur after a small degree of rotation around the N6–C8 bond (as required to realign the O2–H9 bond with the C8 radical center). The other pathway on the S_0 potential-energy surface leads to the diradical intermediate **TD**, which is located 25.4 kcal mol^{-1} in energy below the **CI** point and features a distance of 3.97 Å between the radical centers at C1 and C8. (The relative population of such routes can only be estimated by non-adiabatic dynamics computations that are currently impractical for the model **4**). As mentioned above, free rotation about the N6–C8 and C1–C4 bonds would lead to loss of stereoselectivity. However, as shown in Figure 1, the diradical

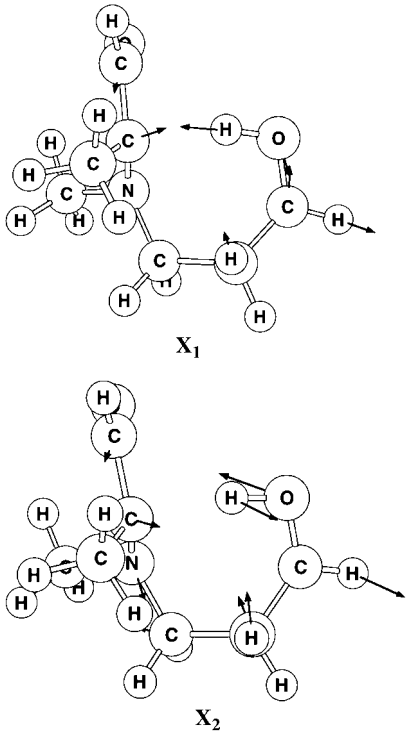

Figure 2. Coordinates X_1 and X_2 that define the "branching" plane along which $S_1 \rightarrow S_0$ decay occurs.

TD is stabilized by a three-center hydrogen bond involving the O12, H9, and N6 atoms, which restrains the conformational freedom of the diradical. Furthermore, diradical disproportionation through the back transfer of the H atom is also restrained by a 9.2 kcal mol^{-1} energy barrier at the transition state **TS-back-H**. This energy barrier results from the large distance (3.19 Å) and unfavorable orientation between the abstracted hydrogen atom and the radical center at C8 imposed by the hydrogen bonds. On the other hand, the orientation of the two carbon-centered radicals at C8 and C1 in the diradical intermediate **TD** is such that cyclization to the product **CP** has a low activation barrier of 5.2 kcal mol^{-1} (**TS-prod**, see Figure 1). Because of the hydrogen-bond network the rotation about N6–C8 required for inversion (or racemization) is slower than the radical coupling, and the original configuration at C8 is thus preserved. The same hydrogen bonds prevent rotation about the C1–C4 bond, so that the *cis* configuration of the hydroxy and aldehyde substituents is favored in the cyclic product. By calculating the energy of nine structures generated by a 20° rotational scan about the C1–O2 bond, the hydrogen-bond strength was estimated to be −5.9 kcal mol^{-1}.[22]

The conclusion that a specific hydrogen-bond network on the S_0 energy surface controls the stereoselectivity of the reaction is supported by reaction-pathway computations for a different, less stable **TD** conformer (6.5 kcal mol^{-1}), indicated as $\mathbf{TD_{conf2}}$, which is not stabilized by two hydrogen bonds (note the long H9–O12 distance of 4.09 Å) as a result of a 180° twisting about C8–C11. The scheme at the bottom of Figure 3 demonstrates that the reaction of this alternative conformer

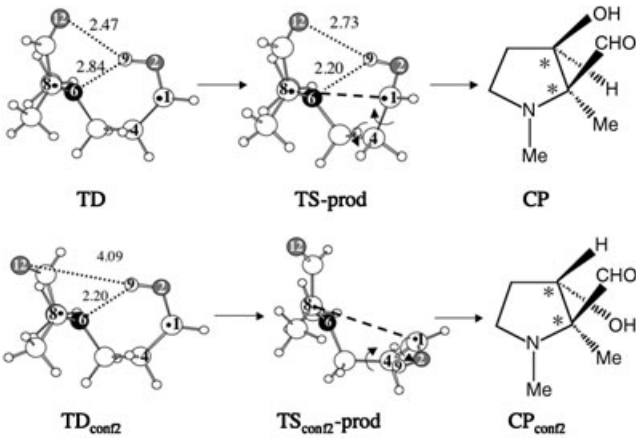

Figure 3. Ground-state reaction routes for two different **TD** conformers of **4** which lead to the *cis* (top) and *trans* (bottom) diastereoisomer of the product; see Figure 1 for atom labels.

generates a $\mathbf{TS_{conf2}}$**-prod** structure, in which the formation of the H9–O12 and H9–N6 hydrogen bonds is impossible. This pathway leads to the minor isomer **3**.

For photoinduced reactions, both the excited- and ground-state branches of the reaction pathway determine the stereoselectivity. Our calculations demonstrate that loss of configuration, through rotation about N6–C8 or C1–C4, can not occur in the excited state. In fact, the transition structure **TS-abst** is cyclic, and the conical intersection **CI** decays to the ground state on a timescale much faster than that of rotation. With regard to the ground-state branch of the reaction, the calculations indicate that the stereoselectivity is determined by the specific structure of the diradical **TD**. In fact, the hydrogen-bond network in **TD** hinders torsional motion about N6–C8 and C1–C4; this torsional motion thus competes inefficiently with cyclization.

Received: September 4, 2004
Revised: January 11, 2005
Published online: March 10, 2005

Keywords: ab initio calculations · chiral memory · conical intersections · photocyclization · reaction mechanisms

[1] A. Córdova, W. Notz, G. Zhong, J. M. Betancort, C. F. Barbas III, *J. Am. Chem. Soc.* **2002**, *124*, 1842.
[2] P. Wessig, P. Wettstein, B. Giese, M. Neuburger, M. Zehnder, *Helv. Chim. Acta* **1994**, *77*, 829.
[3] W. Weigel, S. Schiller, G. Reck, H.-G. Henning, *Tetrahedron Lett.* **1993**, *34*, 6737.
[4] C. Wyss, R. Batra, C. Lehmann, S. Sauer, B. Giese, *Angew. Chem.* **1996**, *108*, 2660; *Angew. Chem. Int. Ed. Engl.* **1996**, *35*, 2529.
[5] K. Nagasawa, A. Georgieva, T. Nakata, *Tetrahedron* **2000**, *56*, 187.
[6] R. Kawecki, *Tetrahedron* **2001**, *57*, 8385.
[7] C. Grison, S. Genève, E. Halbin, P. Coutrot, *Tetrahedron* **2001**, *57*, 4903.
[8] F. Benedetti, M. Magnan, S. Miertus, S. Norbedo, D. Parat, A. Tossi, *Bioorg. Med. Chem. Lett.* **1999**, *9*, 3027.
[9] D. Voet, J. G. Voet, *Biochemie*, VCH, Weinheim, **1992**.

[10] B. Giese, P. Wettstein, C. Stähelin, F. Barbosa, M. Neuburger, M. Zehnder, P. Wessig, *Angew. Chem.* **1999**, *111*, 2722; *Angew. Chem. Int. Ed.* **1999**, *38*, 2586.
[11] A. G. Griesbeck, *Synlett* **2003**, *4*, 451.
[12] P. Celani, M. A. Robb, M. Garavelli, F. Bernardi, M. Olivucci, *Chem. Phys. Lett.* **1995**, *243*, 1.
[13] K. Andersson, M. R. A. Blomberg, M. P. Fülscher, G. Karlström, R. Lundh, P.-A. Malmqvist, P. Neogrády, J. Olsen, B. O. Roos, A. J. Sadlej, M. Schütz, L. Seijo, L. Serrano-Andrés, P. E. M. Siegbahn, P.-O. Widmark, MOLCAS, Version 4, University of Lund, Lund, Sweden, **1997**.
[14] Gaussian 98 (Revision A.7), M. J. Frisch, G. W. Trucks, H. B. Schlegel, G. E. Scuseria, M. A. Robb, J. R. Cheeseman, V. G. Zakrzewski, J. A. Montgomery, R. E. Stratmann, J. C. Burant, S. Dapprich, J. M. Millam, A. D. Daniels, K. N. Kudin, M. C. Strain, O. Farkas, J. Tomasi, V. Barone, M. Cossi, R. Cammi, B. Mennucci, C. Pomelli, C. Adamo, S. Clifford, J. Ochterski, G. A. Petersson, P. Y. Ayala, Q. Cui, K. Morokuma, D. K. Malick, A. D. Rabuck, K. Raghavachari, J. B. Foresman, J. Cioslowski, J. V. Ortiz, B. B. Stefanov, G. Liu, A. Liashenko, P. Piskorz, I. Komaromi, R. Gomperts, R. L. Martin, D. J. Fox, T. Keith, M. A. Al-Laham, C. Y. Peng, A. Nanayakkara, C. Gonzalez, M. Challacombe, P. M. W. Gill, B. G. Johnson, W. Chen, M. W. Wong, J. L. Andres, M. Head-Gordon, E. S. Replogle, J. A. Pople, Gaussian, Inc., Pittsburgh, PA, **1998**.
[15] "Ab initio Methods in Quantum Chemistry-II": B. O. Roos, *Adv. Chem. Phys.* **1987**, *69*, 399.
[16] B. O. Roos, *Acc. Chem. Res.* **1999**, *32*, 137.
[17] Geometry optimization and reaction-path computations were carried out at the CASSCF level of theory with a complete active space including ten electrons in eight orbitals, and the 6-31G* basis set available in Gaussian 98.[13] The orbitals comprise the two σ and σ* C8–H9 orbitals, the four π and π* orbitals of the C1–O2 and C11–012 bonds, and the N6 and O2 lone-pair orbitals. Because of wavefunction instability, the S_0 transition state **TS-back-H** was optimized by using state-average CASSCF with a S_0 and S_1 weight of 0.5. The relaxation coordinates were computed according to the following procedure: 1) The **CI** between the excited state (S_1) and the ground state (S_0) was optimized by using the methodology available in Gaussian 98; 2) the S_0 relaxation pathways were computed starting from the optimized **CI** point by the IRD method, as described in reference [11], and the IRC method available in Gaussian 98. To obtain more-accurate reaction energetics we reevaluated the energy along selected points of the relaxation coordinate at the CASPT2 level by using the program package MOLCAS-4.[12]
[18] H. Ihmels, J. R. Scheffer, *Tetrahedron* **1999**, *55*, 885.
[19] M. Leibovitch, G. Olovsson, J. R. Scheffer, J. Trotter, *J. Am. Chem. Soc.* **1998**, *120*, 12755.
[20] F. Bernardi, M. Olivucci, M. A. Robb, *Chem. Soc. Rev.* **1996**, *25*, 321.
[21] A. Migani, M. Olivucci in *Conical Intersections: Electronic Structure, Dynamics and Spectroscopy* (Eds.: W. Domcke, D. R. Yarkony, H. Köppel), World Scientific, Singapore, **2004**.
[22] If the thermal equilibration of **TD**, kinetic control, and a parallel reaction scheme are assumed, a simple Arrhenius treatment leads to a ratio **2**/**3** of $\exp(E_3-E_2)/RT$, in which E_3 is the barrier to the production of **3** and E_2 is the barrier to the production of **2**. According to this equation, a ratio of 85:15 requires an E_3-E_2 value of approximately 1 kcal mol^{-1}. Thus, if the errors in our computational model are taken into account, the computed value of 0.7 kcal mol^{-1} is consistent with the expected value and with the observed dominance of isomer **2**. Note also that the error associated with the computation of the energy barriers is expected to be close to the value of E_3-E_2.

